

# A Biomathematical Model of Tumor Response to Radioimmunotherapy with $\alpha$ PDL1 and $\alpha$ CTLA4

Isabel González-Crespo, Antonio Gómez-Caamaño, Óscar López Pouso, John D. Fenwick,  
and Juan Pardo-Montero

**Abstract**—There is evidence of synergy between radiotherapy and immunotherapy. Radiotherapy can increase liberation of tumor antigens, leading to activation of antitumor T-cells. This effect can be boosted with immunotherapy. Radioimmunotherapy is therefore a very promising therapeutic combination against cancer, with potential to increase tumor control rates. Biomathematical response models of radioimmunotherapy may help clinicians to design optimal treatment schedules. In this work we present a biomathematical model of tumor response to radioimmunotherapy. The model uses the linear-quadratic response of tumor cells to radiation, and builds on previous developments to include the radiation-induced immune effect. We have focused this study on the combined effect of radiotherapy and  $\alpha$ PDL1/ $\alpha$ CTLA4 therapies. The model fits recent preclinical data of volume dynamics and control obtained with different dose fractionations and  $\alpha$ PDL1/ $\alpha$ CTLA4. A biomathematical study of optimal combination strategies suggests that a good understanding of the biological delays associated to radioimmunotherapy, the biokinetics of the immunotherapy drug, and the interplay among them, may be of paramount importance to design optimal radioimmunotherapy schedules. Biomathematical models like the one we present can help to interpret experimental data on the synergy between radiotherapy and immunotherapy, and to assist in the design of more effective treatments, could potentially boost the implementation of radioimmunotherapy.

**Index Terms**—Radioimmunotherapy, radiotherapy,  $\alpha$ PDL1,  $\alpha$ CTLA4, biomathematical modeling.

## 1 INTRODUCTION

TUMOR cells present antigens that can be recognized by the immune system. Cancer immunotherapy (IT) is a therapeutic strategy against cancer that aims at boosting and exploiting the natural immune response to control and cure tumors [1], [2]. Drugs approved for therapy include specific antibodies against tumor antigens, especially membrane receptors, which activate an immune response that can lead to cell death. Several antibodies have been approved for treatment of cancer, including melanoma, prostate, NSCLC and leukemia [3], [4], [5], [6], [7]. CTLA-4 is a down-regulator of immune response, and antibodies aiming at inactivating CTLA-4 increases immune response. PD-1 and PD-L1 are also well known suppressors of the immune response against tumors. Inhibitors of these proteins have shown promising results in preclinical experiments, and there are several monoclonal antibodies against PD-1/PD-L1 approved for treatment several types of cancer [8]. How-

ever, efficacy of IT as cancer treatment is still limited, but for particular cases. For example, ipilimumab has shown an improvement on the survival of melanoma patients, but response rates are low, in the 10-15% range [9].

In the last few years several experimental results have shown the synergy of combining IT with radiotherapy [10], [11], [12], [13]. Radiotherapy (RT) is a cancer therapy that consists in delivering a high dose of radiation to the tumor, while keeping radiation doses received by nearby organs within tolerance levels. The dominant biological cell killing mechanism behind the effect of RT is the generation of double strand breaks in the DNA by ionizing particles [14]. However, there is evidence that radiation can trigger other cell killing mechanisms, particularly when delivered at high-doses per fraction, which are especially important for the synergy with immunotherapy. High-doses of radiation can damage the tumor vascular system, eventually triggering cell death [15], and high-doses can also trigger an immune response against surviving tumor cells [11], [16], [17], increasing the likelihood of tumor control. The mechanisms behind these induced immune effect seem to be related to the increased liberation of tumor antigens, which cause the activation of antitumor T cells, and the modification of the tumor microenvironment, killing immune down-regulators like Treg and MDSC cells, and facilitating T cell infiltration in the tumor [18], [19], [20]. Many preclinical studies have shown that the combination of RT with inhibitors of CTLA-4, PD-1 and PD-L1 is significantly more effective than RT and IT alone [19], [21], [22].

Despite the potential of IT and RT, how the best combination of both therapies can be achieved is still a matter of study. In this regard, validated biomathematical models of RT+IT (*in silico* tumor models) would be very useful. Bioma-

• *I. González-Crespo is with the Group of Medical Physics and Biomathematics, Instituto de Investigación Sanitaria de Santiago, Spain.*

• *A. Gómez-Caamaño is with the Department of Radiation Oncology, Clinical University Hospital of Santiago, Spain.*

• *Ó. López Pouso is with the Group of Medical Physics and Biomathematics, Instituto de Investigación Sanitaria de Santiago, and the Department of Applied Mathematics, Universidad de Santiago de Compostela, Spain.*

• *J.D. Fenwick is with the Department of Molecular and Clinical Cancer Medicine, Institute of Translational Medicine, University of Liverpool, Liverpool, United Kingdom.*

• *J. Pardo-Montero is with the Group of Medical Physics and Biomathematics, Instituto de Investigación Sanitaria de Santiago, Spain. E-mail: juan.pardo.montero@sergas.es*

themtical models, based on solid experimental and clinical data are of high importance in order to interpret results, and may also assist on the design of optimal therapeutic strategies, potentially guiding clinicians in the selection of optimal treatments (similarly to the role of the linear-quadratic model in radiotherapy). Modeling the response of tumors to IT has been addressed in the biomathematical modeling literature, following both phenomenological and systems biology approaches [23], [24], [25], [26], [27], [28], [29]. On the other hand, modeling the synergistic combination of IT and RT has been less studied due to the novelty of this treatment strategy, but it is becoming an active field of research [30], [31], [32], [33], [34], [35]. We would like to highlight the recent works of Serre et al. and Kosinsky et al. [30], [31], [32]. In the former paper, a simple model of response to radioimmunotherapy with inhibitors of CTLA-4 and PD-L1 is presented and used to fit experimental data of tumor response and rejection probability of implanted tumors. The latter study presents a more complicated model, based on ordinary differential equations, which is used to fit experimental data and to formulate hypothesis of optimal treatment strategies with RT+inhibitors of PD-L1.

In this work we build upon these works to develop a dynamical model of tumor response to radioimmunotherapy with inhibitors of PD-L1 ( $\alpha$ PDL1) and CTLA-4 ( $\alpha$ CTL4). The model consists in a system of coupled impulsive delay-differential equations (DDE) that describe the time evolution of the most relevant populations of cells. DDE are used to explicitly include biological response delays, which may have importance when modeling biological systems. The model is presented both as a continuous deterministic model and as a discrete stochastic *Markov-birth-death* model (the latter formulation is specially important when modelling control (or lack of thereof)). The model has been validated by fitting experimental preclinical data of tumor response to combined therapies of radiation, with different fractionations, and  $\alpha$ PDL1/ $\alpha$ CTL4 [21], [22], including volume dynamics and tumor control.

## 2 METHODS AND MATERIALS

### 2.1 Overview of the Model

Our biomathematical model follows the cancer-immunity cycle [18], presented in Fig. 1(A) together with sketches of the role of  $\alpha$ CTL4, Fig. 1(B), and  $\alpha$ PDL1, Fig. 1(C). A sketch of the biomathematical model is shown in Fig. 1(D). Tumor cells release antigens, naturally and due to cell death; antigens are taken by antigen-presenting-cells (APCs) to activation sites (lymph nodes) where they trigger T-cell activation; active T-cells migrate to the tumor, infiltrate it, and kill tumor cells. Each radiation dose fraction kills tumor cells (contributing to the release of antigens), as well as T-cells present in the tumor. Immunotherapy drugs affect either the activation of T-cells ( $\alpha$ CTL4) or the tumor cell-killing by activated T-cells ( $\alpha$ PDL1). The model includes three main species: tumor cells, T-cells, and antigens/APCs. These species are split into six different compartments, which exist in two different spatial locations: in the tumor (viable tumor cells,  $N$ ; tumor cells that are doomed by radiation and will eventually die,  $N_d$ ; active T-cells against tumor cells,  $L$ ), and in the activation sites (a phenomenological compartment  $A$

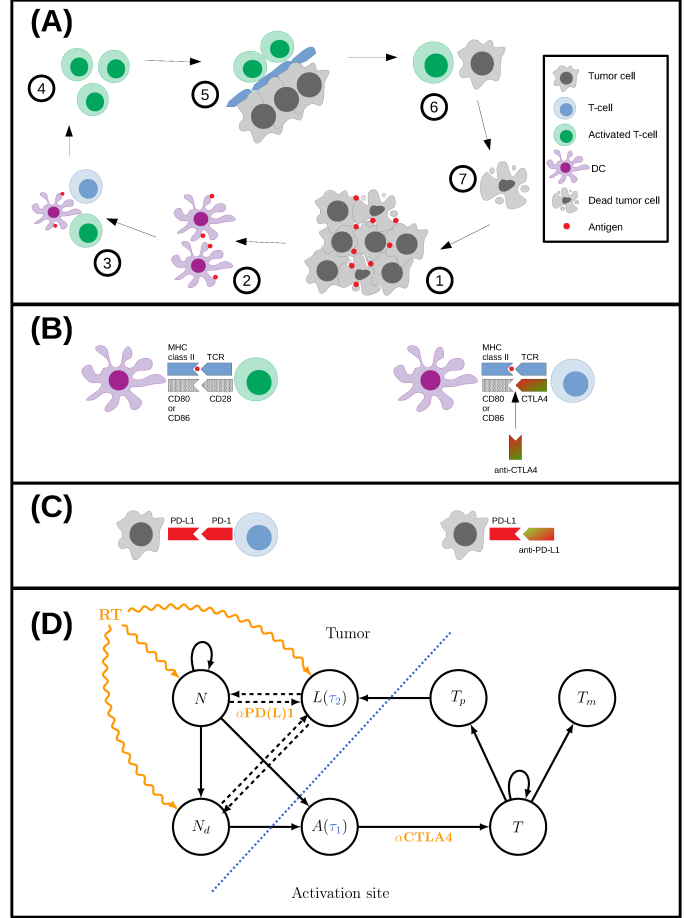


Fig. 1. Sketch of the tumor immunity cycle and the role of  $\alpha$ PDL1/ $\alpha$ CTLA4, that serves as the basis for our mathematical model, and sketch of the flowchart of the biomathematical model. (A) Sketch of the tumor immunity cycle: 1) Tumor cells release antigens, either naturally or responding to radiotherapy damage; 2) dendritic cells take antigens to activation sites (lymph nodes); 3) T-cells against tumor cells are activated; 4) T-cells migrate to the tumor and 5) infiltrate it; 6) T-cells attack tumor cells and 7) kill them. (B) Sketch of T-cell activation blocking by the CTLA-4 receptor, and the potential role of  $\alpha$ CTLA4. (C) Sketch of the inactivation of T-cells through the PD-L1 receptor, and role of  $\alpha$ PDL1 in avoiding such inactivation. (D) Sketch of the flowchart of the model showing interconnections between different compartments: viable tumor cells ( $N$ ), doomed tumor cells ( $N_d$ ), active T-cells in the tumor ( $L$ ), antigens/APCs ( $A$ ), as well as pool of T-cells ( $T$ ), activated T-cells ( $T_p$ ) and blocked T-cells ( $T_m$ ). The dashed line shows the separation between compartments physically located in the tumor (left) and compartments physically located in activation sites.  $\tau_1$  and  $\tau_2$  are biological delays for migration between those two physical locations. The effect of radiotherapy (RT), and  $\alpha$ PDL1/ $\alpha$ CTLA4 is also indicated.

accounting for the effects of antigens and APCs; the T-cell pool,  $T$ ; activated T-cells,  $T_p$ ; blocked T-cells  $T_m$ ). Migration between different spatial locations (antigens/APCs migrating from the tumor to activation sites and activated T-cells migrating from the activation sites to the tumor) will result in a biological delay which will be explicitly included in our model by using delay differential equations. The effect of radiation dose delivery is treated as an impulse (thus, formally, the differential equation are impulsive) The main terms involved in the dynamics of our model can be shown

in a simple way as:

$$\begin{aligned}
 \text{dynamics } N &= \text{proliferation} - \text{radiation death} \\
 &\quad - \text{immune death} \\
 \text{dynamics } A &= \text{natural release} + \text{radiation-mediated release} \\
 &\quad - \text{natural elimination} - \text{T-cell activation} \\
 \text{dynamics } L &= \text{activation/infiltration} - \text{radiation death} \\
 &\quad - \text{immune death} - \text{natural elimination}
 \end{aligned}$$

The model is built following a mechanistic approach rather than a purely phenomenological approach. It includes many simplifications, though, in order to present a tractable problem. Among the most relevant simplifications, we should cite: i) We do not include spatial coordinates in our multi-compartmental model; ii) The process of immune death is overly simplified. In particular, we do not include other cell types that participate in this process, either favoring immunity or acting as suppressors, like natural killers or T-reg; iii) We mostly rely on the linear-quadratic model (LQ) to account for radiation cell death, but departures from the LQ model at high-doses are studied and discussed.

## 2.2 Direct Cell Death and Kinetics

Dose delivery is modeled as instantaneous (the instantaneous dose delivery seems like a good approximation, as in typical fractionated treatments it takes minutes, while the typical times of our model are days). Radiation tumor cell death is modeled with the linear-quadratic (LQ) model:

$$\log SF = -\alpha d - \beta d^2 \quad (1)$$

where  $SF$  is the surviving fraction of a population of cells after being irradiated to a radiation dose,  $d$ , and  $\alpha$  and  $\beta$  are the LQ linear and quadratic parameters.

We will fit data with different fractionation schedules. It is well known that cell death can depart from the standard LQ-model, especially at high doses per fraction. Several effects contribute to this: re-oxygenation (which leads to radiosensitization) depending on the dose per fraction [36], saturation [37], or vascular damage [15]. As those effects apply mostly to the LQ model's, yet it is still not known how much, we have checked whether a simple ad hoc modification of the quadratic term can change the goodness of the fit [38]:

$$\beta_N \rightarrow \beta_{N_0} \left( 1 + c\sqrt{d} \right) \quad (2)$$

where  $c$  is a free parameter,  $d$  is the dose per fraction, and the  $\sqrt{d}$  dependence was used to have a moderate dependence on the delivered radiation dose.

We will also use the Linear-Quadratic-Linear (LQL) model [39], which models the surviving fraction as:

$$\log SF = -\alpha d - 2\beta \frac{xd - 1 + e^{-xd}}{x^2} \quad (3)$$

Here  $x$  is an extra parameter that shapes the slope of the curve. We will use these expressions to model both radiation-induced tumor cell and T-cell death, but with different parameters. The modification of the term  $\beta$  is only employed for tumor cells.

Cells fatally damaged by radiation (doomed) do not die instantly, but follow a given kinetics, generally a pause

(mitotic delay) followed by a progressive death as lethally damaged cells entering mitosis and suffer mitotic catastrophe. We will model that effect by considering a mitotic delay followed by an exponential death [40].

Viable tumor cells can proliferate, and we describe this using the logistic formalism [41]. On the other hand, while doomed cells may carry some proliferative capacity (abortive divisions [42]), it should be limited and does not contribute to the long-term cell population, and we will ignore it.

From the above considerations we can write the following equation for viable tumor cells:

$$\frac{dN}{dt}(t) = \lambda_1 N(t)[1 - \lambda_2(N(t) + N_d(t)) - K_N(t)N(t)] \quad (4)$$

where  $\lambda_1, \lambda_2$  are constants.  $K_N(t)$  is an impulse accounting for the effect of the radiation dose:

$$K_N(t_i) = \begin{cases} 0, & \text{if } t_i \notin \{t_k\} \\ (1 - SF_N(d_i)), & \text{if } t_i \in \{t_k\} \end{cases} \quad (5)$$

where  $\{t_k\}$  is vector of radiation delivery times,  $d_i$  is the dose delivered at time  $t_i$ , and  $SF_N$  is the surviving fractions of tumor cells given by (1), (2) or (3).

For doomed cells, we will consider that each radiation fraction will create new doomed cells, but will not interfere with the radiation kinetics of existent doomed cells. Therefore, we can split the compartment of doomed cells into  $n$  compartments of doomed cells created by  $n$  dose fractions:

$$\frac{dN_{d,i}}{dt}(t) = K_N(t)N(t) - \phi\omega(\bar{t}_i)N_{d,i}(t) \quad (6)$$

$$N_d(t) = \sum_i N_{d,i} \quad (7)$$

Here,  $N_{d,i}(t)$  denotes doomed cells created by radiation  $i$ ,  $t_i$  is the delivery time of that fraction, and  $\bar{t}_i = t - t_i$ . Notice that  $N_{d,i}(t)$  as defined is zero for  $t < t_i$ . On the other hand,  $\phi$  is the death rate, and  $\omega$  models the mitotic delay and progressive incorporation of damaged cells to cell death kinetics after a radiation fraction:

$$\omega(\bar{t}) = \begin{cases} 0, & \text{for } \bar{t} \leq \tau_{d1} \\ \frac{\bar{t} - \tau_{d1}}{\tau_{d2} - \tau_{d1}}, & \text{for } \tau_{d1} < \bar{t} \leq \tau_{d2} \\ 1, & \text{for } \bar{t} > \tau_{d2} \end{cases} \quad (8)$$

On the other hand, radiation will also kill T-cells present in the tumor as:

$$\frac{dL}{dt}(t) = -K_L(t)L(t) \quad (9)$$

Where  $K_L(t)$  is the impulse term for T-cells, which has the same form of (5), but with  $SF_L$ , the surviving fraction of T-cells. It is assumed that radiation-damaged T-cells die instantly, and so there are no kinetics associated to such death.

### 2.3 Antigen Release and T-cell Activation

Antigens are considered to be released both naturally (rate proportional to the number of tumor cells, both viable and doomed), and during radiation-induced cell death (proportional to the rate of cell death). In addition, we include a term describing natural elimination. As the compartment  $A$  is located in the T-cell activation sites, a biological delay  $\tau_1$  is included to account for migration from the tumor:

$$\begin{aligned}\frac{dA}{dt}(t) &= \rho(N(t - \tau_1) + N_d(t - \tau_1)) \\ &+ \psi\phi\omega(\bar{t} - \tau_1)N_d(t - \tau_1) - \sigma A(t)\end{aligned}\quad (10)$$

The activation of T-cells against tumor cells is modeled through four bilinear equations which describe the generation of activated T-cells ( $T_p$ ) or inactivated T-cells ( $T_m$ ) (through the CTLA-4 receptor) from a pool of blank T-cells ( $T$ ):

$$\frac{dA}{dt}(t) = -aA(t)T(t) - bA(t)T(t) \quad (11)$$

$$\frac{dT}{dt}(t) = -aA(t)T(t) - bA(t)T(t) + h \quad (12)$$

$$\frac{dT_p}{dt}(t) = aA(t)T(t) \quad (13)$$

$$\frac{dT_m}{dt}(t) = bA(t)T(t) \quad (14)$$

The constants  $a$  and  $b$  ( $r = 1 + b/a$ ) describe the affinities for activation/inactivation, respectively [30]. The pool of blank T-cells is assumed to renew at constant rate (due to maturation of new T-cells),  $h$ . Active T-cells migrate to the tumor (biological delay  $\tau_2$ ) where they become part of the compartment  $L$ :

$$\frac{dL}{dt}(t) = \frac{dT_p}{dt}(t - \tau_2) = aA(t - \tau_2)T_p(t - \tau_2) \quad (15)$$

We have tested the hypothesis that vascular damage at high radiation doses may affect the effectiveness of radioimmunotherapy by limiting the infiltration of T-cells in the tumor. We have included a dose and time dependent T-cell infiltrating parameter in our model, equation (15), to account for vascular damage and recovery. Inspired by [15], [43], we consider critical vascular damage doses beyond 15 Gy, and a progressive recovery of function as:

$$f(t) = \min\{0.05t, 1\} \quad (16)$$

where the time post-irradiation  $t$  is measured in days. This factor represents the fraction of active T-cells reaching the tumor, and multiplies (15).

### 2.4 T-cell Mediated Tumor Cell Death

Interaction between active T-cells and tumor cells will result in the partial depletion of both compartments. Following the work of de Pillis et al. [23], we model this interaction with a bilinear term for the compartment  $L$ , in addition to an exponential natural elimination:

$$\frac{dL}{dt}(t) = -\iota L(t)(N(t) + N_d(t)) - \eta L(t) \quad (17)$$

On the other hand, T-cell mediated tumor cell death is modeled with the following term [23]:

$$\frac{dN}{dt}(t) = -p \frac{(L(t)/N(t))^q}{s + (L(t)/N(t))^q} N(t) \quad (18)$$

The same expression holds for  $N_d(t)$ . Note that this terms add into earlier equations.

### 2.5 The Effect of $\alpha$ PDL1 and $\alpha$ CTLA4

The biokinetics of concentrations (in arbitrary units) of  $\alpha$ PDL1 ( $p_1$ ) and  $\alpha$ CTLA4 ( $c_4$ ) is modeled as an instantaneous source term at injection times ( $\{t_{p1}\}$  or  $\{t_{c4}\}$ ) and a continuous exponential elimination:

$$\frac{dc_4}{dt}(t) = i_{c4}(t)\delta(t - \{t_{c4}\}) - \nu c_4(t) \quad (19)$$

$$\frac{dp_1}{dt}(t) = i_{p1}(t)\delta(t - \{t_{p1}\}) - \mu p_1(t) \quad (20)$$

The precise pharmacokinetic modeling of these drugs is beyond the scope of the present article. However, this seems a good approximation for the kinetics of  $\alpha$ CTLA4: Selby et al. [44] investigated the biokinetics of different  $\alpha$ CTLA4 drugs, finding that they follow linear kinetics like (19). On the other hand, Deng et al. [45] investigated the biokinetics of  $\alpha$ PDL1, finding more complex kinetic, non-linear, behaviour.

Rather than considering a complex kinetics model for the characterization of the effect of  $\alpha$ CTLA4 on the activation of T-cells, we model the effect as a simple dependence of the parameter  $b$  in (11), (12) and (14) on  $c_4$ , similarly to [30]:

$$b \rightarrow \frac{b}{1 + c_4(t)} \quad (21)$$

On the other hand, the effect of  $\alpha$ PDL1 on the immune-death of tumor cells is modeled by introducing a dependence of the parameter  $p$  in (18) as:

$$p \rightarrow p(1 + p_1(t)) \quad (22)$$

### 2.6 The Complete Model

The assembled model has the following form for compartments  $N$ ,  $N_d$ ,  $A$  and  $L$ :

$$\begin{aligned}\frac{dN}{dt}(t) &= \lambda_1 N(t) \left( 1 - \lambda_2 \left( N(t) + \sum_i N_{d,i}(t) \right) \right) \\ &- K_N(t)N(t) - p(1 + p_1(t)) \frac{(L(t)/N(t))^q}{s + (L(t)/N(t))^q} N(t) \\ \frac{dN_{d,i}}{dt}(t) &= K_N(t)N(t) - \omega(\bar{t}_i)\phi N_{d,i}(t) \\ &- p(1 + p_1(t)) \frac{(L(t)/N_{d,i}(t))^q}{s + (L(t)/N_{d,i}(t))^q} N_{d,i}(t) \\ \frac{dL}{dt}(t) &= -K_N L(t) + aA(t - \tau_2)T_p(t - \tau_2) \\ &- \iota L(t) \left( N(t) + \sum_i N_{d,i}(t) \right) - \eta L(t) \\ \frac{dA}{dt}(t) &= \rho \left( N(t - \tau_1) + \sum_i N_{d,i}(t - \tau_1) \right) \\ &+ \psi\phi \sum_i \omega(\bar{t}_i - \tau_1)N_{d,i}(t - \tau_1) - \sigma A(t) \\ &- aA(t)T(t) - \frac{b}{1 + c_4(t)} A(t)T(t)\end{aligned}\quad (23)$$

In addition, (12)-(14) control the activation of T-cells against tumor cells, and (19, 20) control the bio-kinetics of  $\alpha$ PDL1 and  $\alpha$ CTLA4.

## 2.7 Modeling Tumor Control Probability: Markov model

We have employed the *clonogenic cell hypothesis* [46] to obtain tumor control probabilities (TCP) from our model. Such hypothesis states that in order to control the tumor, all cells with proliferative capacity need to be eliminated, which we identify with the compartment  $N$  in our model. Our model, as defined in the previous section, is continuous and deterministic. In order to model TCP we need a discrete (numbers of cells) and stochasticity. Therefore, for low numbers of cells ( $N < 1000$  cells), the model was converted to a Markov birth/death stochastic process [47] by interpreting terms in the differential equations as birth/death probabilities. In a simulation, the tumor was considered controlled if  $N$  reaches 0. In addition to the stochasticity of the Markov model, in order to obtain populational TCPs we also implemented random perturbations of the model parameters to simulate the heterogeneity of a population, and:

$$TCP = \frac{\text{number of controls}}{\text{number of simulations}} \quad (24)$$

Confidence intervals for TCP values are obtained by using the Clopper-Pearson methodology.

## 2.8 Experimental Data

In [21] the authors studied the response of tumors in mice to radiotherapy (different fractionations) and  $\alpha$ CTLA4, either as monotherapies or in combination. Tumor cells were planted on the side of mice and let grow for 12 days, when they reached a volume  $\sim 32 \text{ mm}^3$ . Treatments started at that time, and evolution of tumor volumes were monitored every 3 days. They studied tumor response to different combinations of RT+IT. In particular: **i**) no treatment; **ii**) RT alone, 20 Gy single-fraction; **iii**) RT alone, 3 fractions of 8 Gy (days 12, 13 and 14); **iv**) RT alone, 5 fractions of 6 Gy (days 12, 13, 14, 15, and 16); **v**) IT alone, delivered in 3 fractions (days 14, 17, 20); **vi**) combined RT+IT, 20 Gy + 3 fractions of IT (ii+v); **vii**) combined RT+IT, (6 Gy  $\times$  5) + 3 fractions of IT (iv+v); **viii**) combined RT+IT, (8 Gy  $\times$  3) + 3 fractions of IT (iii+v); **ix**) combined RT+IT, (8 Gy  $\times$  3) + 3 fractions of IT at days 12, 15, 18; **x**) combined RT+IT, (8 Gy  $\times$  3) + 3 fractions of IT at days 16, 18, 20. In addition, this article also reported the fraction of animals where tumor control was achieved (TCP).

In [22] the authors present responses of tumors to radiotherapy and  $\alpha$ PDL1. Tumor cells were implanted in mice, and tumors were allowed to grow for 14 days, when they had volumes around  $100 \text{ mm}^3$ . At that time, treatments started and tumor volumes were monitored up to day 35. The different experimental arms are: **i**) no treatment; **ii**) single dose of 12 Gy; **iii**) four fractions of  $\alpha$ PDL1 at days 14, 17, 20 and 23; **iv**) 12 Gy +  $\alpha$ PDL1 (ii+iii).

In order to fit the reported evolution of tumor volumes, firstly, we let the modeled tumors to freely grow until they reached the relevant pre-treatment volumes reported in [21] and [22]. That time was defined as reference (day 0), and treatment times are defined relative to that time. Notice that the time to reach those volumes differs from the experimental results, as we start with different numbers of cells than those experimentally injected and our model does

not aim to describe the biophysics of tumor growth, which may be dominated by different mechanisms than tumor response.

Tumor volumes in our model are computed by considering the populations of both tumor cells (viable and doomed) and T-cells in the tumor. Therefore:

$$V_{\text{model}} = [N(t) + N_d(t)]V_N + L(t)V_L \quad (25)$$

where  $V_N$  and  $V_L$  are the volumes of individual tumor cells and T-cells respectively.

A simulated annealing method [48] was implemented to find best fitting parameters. The objective function to be minimized is the weighted sum of square differences between model and experimental values:

$$F = \sum_{\text{curves points}} \sum \frac{(V_{\text{model}} - V_{\text{exp}})^2}{u^2} \quad (26)$$

where  $V_{\text{exp}}$  and  $V_{\text{model}}$  are the experimental and model results, and  $u$  are the experimental uncertainties. The optimization method has been applied to all response curves in each experiment at once (i.e. the sum above runs over different time points and different combinations of radiotherapy and immunotherapy), to avoid different best-fitting parameters for each curve.

## 2.9 Biologically Effective Dose

The biologically effective dose (BED) [49] was used to design different radiobiologically iso-effective fractionations. The BED of a schedule delivering a total dose  $D$  in fractions of dose  $d$  is given by:

$$BED = D \left( 1 + \frac{d}{\alpha/\beta} \right) \quad (27)$$

where  $\alpha/\beta$  is the ratio of the linear and quadratic terms in the LQ model.

## 2.10 Qualitative Sensitivity Analysis

We have performed a qualitative local parametric sensitivity analysis. In order to do so, we have evaluated the sensitivity of the cost function to parameter perturbations around best-fitting values by approximating the derivative of the cost function as,

$$S_i = |F(\mathbf{x}) - F(\mathbf{x} + \Delta x_i)| \simeq \left| \frac{\partial F}{\partial x_i} \right| h_i \quad (28)$$

where  $F$  is the cost function (26),  $\mathbf{x}$  is the set of best-fitting parameters and  $\Delta x_i = (0, \dots, 0, h_i, 0, \dots)$ .  $h_i$  was set to 1% of the best-fitting value  $x_i$ .

## 2.11 Implementation and Parameters

The model was implemented in different routines in Matlab (The Matworks, Natick, MA). The model is solved by employing an explicit Euler method [50], with a time step of 0.05 days. The main routines and the data used for model fitting are available from the Dataverse repository [51].

Not all model parameters were free during the fit to experimental data. Cell volumes in (25) were set to  $V_N = 10^{-6} \text{ mm}^3$  and  $V_L = 2 \times 10^{-7} \text{ mm}^3$  [52]. For the radiosensitivity of T-cells we have constrained the  $\beta$ -term

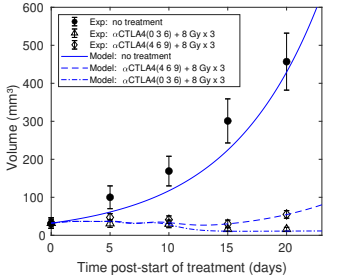
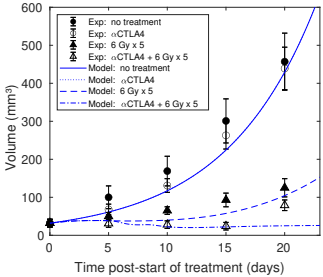
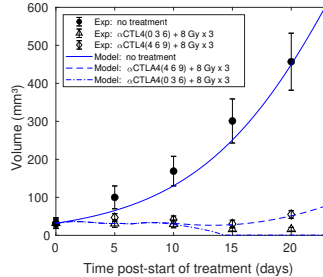
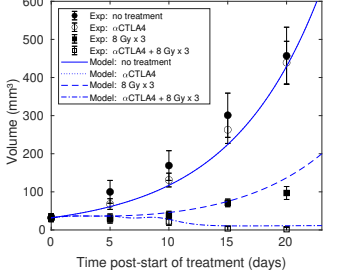
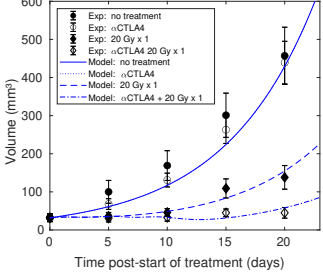
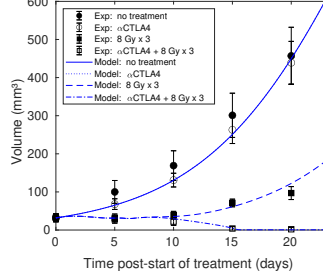
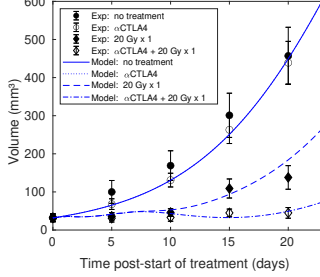


Fig. 2. Model fitting of experimental data reported by Dewan et al. [21] of tumor response to radiotherapy, immunotherapy with  $\alpha$ CTLA4, and combined treatment. Radiation doses are delivered in consecutive days starting from day 0, and immunotherapy doses are delivered at days (2, 5, 8) unless specified otherwise. Notice that differences between model curves for "no treatment" and " $\alpha$ CTLA4" are small and both curves overlap in the figure.

as  $\beta_L = \alpha_L/10$ . The biokinetic elimination of  $\alpha$ PDL1 and  $\alpha$ CTLA4 were set to  $\mu = 0.5$  and  $\nu = 0.1 \text{ days}^{-1}$ , from fits to data reported in [44], [45]. The parameters characterizing the mitotic delay of radiation-damaged cells were set to  $\tau_{d1} = 1 \text{ days}$ ,  $\tau_{d2} = 1.5 \text{ days}$ , which is in the range of reported mitotic delays. On the other hand, values of best-fitting parameters were constrained when necessary (for example,  $\alpha > 0$  and  $\beta > 0$  in the LQ-model, or  $\lambda > 0$  for tumor proliferation).

### 3 RESULTS

#### 3.1 The Model Can Fit Pre-clinical Data of Tumor Response to Combined Therapies of Radiation and $\alpha$ PDL1/ $\alpha$ CTLA4

In Fig. 2 we report best fits of our model to volume dynamics data presented in [21]. In this dataset, when no treatment is delivered, tumor volume presents an exponential-like growth,  $\alpha$ CTLA4 alone has not significant effect on tumor response (evolution of tumor volume with time), RT alone causes a moderate tumor response, and the combination of RT and  $\alpha$ CTLA4 causes an important tumor response, achieving tumor control in some cases (for 8 Gy  $\times$  3). Our model can reproduce these progression patterns, as shown in Fig. 2. Best-fitting parameters are presented in Supplementary Table 1.

Data fitting point to a decrease in relative radiosensitivity with increasing dose (negative parameter  $c$  in (2)). Such behavior can be described by the LQL model. Therefore, we have performed the same fit with the LQL instead of the modified LQ model (Fig. 3), obtaining similar results (best-fitting parameters reported in Supplementary Table 2).

Fig. 3. Model fitting of experimental data reported by Dewan et al. [21] of tumor response to radiotherapy, immunotherapy with  $\alpha$ CTLA4, and combined treatment. The LQL model was used to account for the radiosensitivity of tumor cells. Radiation doses are delivered in consecutive days starting from 0, and immunotherapy doses are delivered at days (2, 5, 8) unless specified otherwise. Notice that differences between model curves for "no treatment" and " $\alpha$ CTLA4" are small and both curves overlap in the figure.

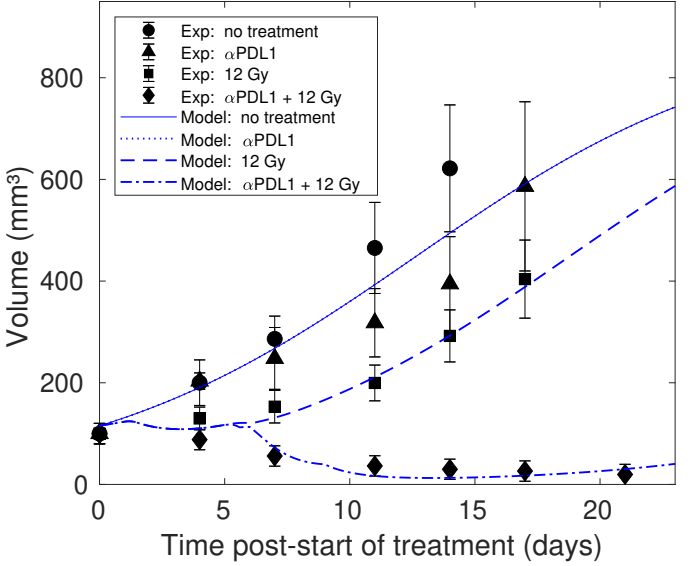


Fig. 4. Model fitting of experimental data reported by Deng et al. [22] of tumor response to radiotherapy (12 Gy  $\times$  1 fraction), immunotherapy with  $\alpha$ PDL1, and combined treatment. Notice that differences between model curves for "no treatment" and " $\alpha$ PDL1" are small and both curves almost overlap in the figure.

In Fig. 4 we report best fits of our model to data presented in [22], which shows tumor responses to radiotherapy and  $\alpha$ PDL1. This dataset presents similar patterns of tumor response:  $\alpha$ PDL1 alone has not significant effect on tumor response, RT alone causes a moderate tumor response, and the combination of RT+ $\alpha$ PDL1 presents synergy and leads to an important tumor response.

Best-fitting parameters are reported in Supplementary

Table 1. To fit data of Fig. 4 we have kept fixed most of the best-fitting parameters obtained when fitting Fig. 2: only parameters related to the kinetics of  $\alpha$ PD1, tumor cell proliferation and tumor cell radiosensitivities ( $\alpha$  and  $\beta$  in the linear-quadratic model) were allowed to vary. While there are differences in the clones and tumors that could justify using different host-related and tumor-related parameters, we think that imposing such constraints on the optimization poses a serious test to our model, and avoids reaching good fits by over-fitting.

Volumes presented in previous figures include tumor cells and T-cells. Certainly, we do not want our model to reproduce tumor volumes by including large fractions of T-cells and low fractions of tumor cells, which would eventually lead to tumor control, and would contradict experimental evidence. In Supplementary Fig. 1 and Supplementary Fig. 2 we present the contribution of tumor cells and T-cells to tumor volumes, and show that modeled tumor volumes are dominated by tumor cells.

### 3.2 Vascular Damage May Limit the Effectiveness of Radioimmunotherapy

Large radiation doses can seriously damage tumor vasculature, which may also limit the infiltration of active T-cells in the tumor. This might also explain the poorer results obtained with the 20 Gy single-fraction irradiation in [21]. In order to test the hypothesis that vascular damage may affect the effectiveness of radioimmunotherapy, we removed the dependence of the tumor cells  $\beta$ -term on radiation dose (see Section 2.2), and we included a dose and time dependent T-cell infiltrating parameter in our model (16), to account for vascular damage and recovery. Inspired by [15], [43], we consider critical vascular damage for irradiation with 20 Gy, followed by a progressive recovery of vascular function. This factor represents the fraction of active T-cells reaching the tumor.

In Fig. 5 we show best fits of our model to that dataset. The model provides a good fit to the experimental values. The goodness of the fit is not significantly different from that reported in Fig. 2. Best-fitting model parameters for this case are shown in Supplementary Table 3.

### 3.3 Optimizing the Schedule of Administration of Radiotherapy and Immunotherapy Can Improve Effectiveness

Finding the optimal sequence of administration of IT+RT can improve effectiveness, as experimentally shown in results presented in [21]. This may be caused by the interplay between biological mechanisms with different kinetics, including the biological delays arising from the release of antigens to the activation of T-cells, and the migration of such T-cells to the tumor, tumor proliferation, and the progressive death of doomed cells.

We have investigated this effect for the combined RT+IT treatment with  $(8 \text{ Gy} \times 3) + 3$  fractions of  $\alpha$ CTLA4, reported in [21]. We have used the best-fitting parameters reported in Supplementary Table 3. In order to simulate population tumor control probabilities, we have used the stochastic Markov model described in Section 2.7, together with a relative normal random dispersion of best-fitting parameters

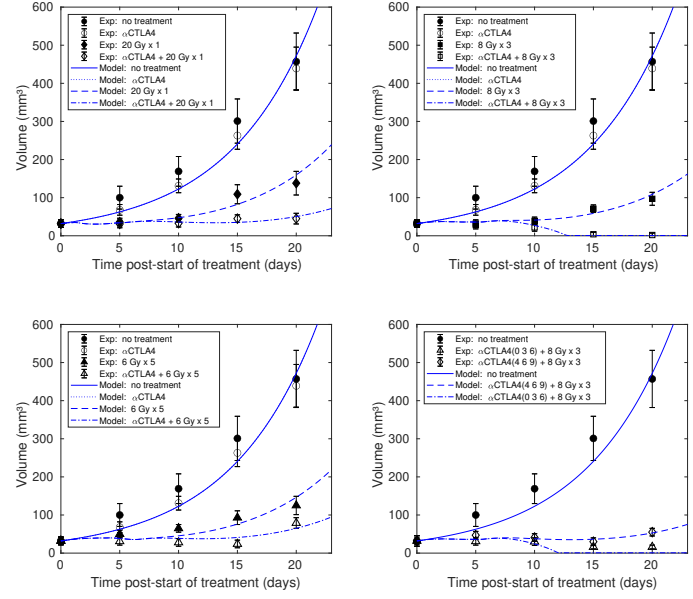


Fig. 5. Model fitting of experimental data reported by Dewan et al. [21] of tumor response to radiotherapy, immunotherapy with  $\alpha$ CTLA4, and combined treatment. The classical LQ model is used to characterize tumor cell response to radiation, and vascular damage at 20 Gy per fraction is included to limit T-cell infiltration in the tumor. Radiation doses are delivered in consecutive days starting from 0, and immunotherapy doses are delivered at days (2, 5, 8) unless specified otherwise. Notice that differences between model curves for "No treatment" and " $\alpha$ CTLA4" are small and both curves overlap in the figure.

of 10% (to simulate population heterogeneity). The days of administration of radiotherapy were kept fixed (0, 1 and 2 days), and the days of administration of IT were varied, starting from day 0 to day 7 (thus ending from day 2 to day 9). The evolution of tumor volumes and the TCP was evaluated for each treatment configuration from 200 simulations.

Results are reported in Fig. 6. In Fig. 6(A)-(C) we report the dynamics of tumor volumes (mean  $\pm$  1 standard deviation) for three combinations that were investigated in [21]. In Fig. 6(D) we compare 95% confidence intervals for TCP values obtained with the model (200 simulations) and experimental controls (6 to 21 animals), for the same three treatment combinations. Finally, In Fig. 6(E) we present model TCPs versus the time of administration of the first IT fraction, showing that there is a negative correlation between those two variables if IT is delayed beyond two days post-start of RT.

### 3.4 Optimal Dose Fractionation Can Improve Effectiveness Of Radioimmunotherapy

With the set of parameters shown in Supplementary Table 3 we have studied the combined effect of different fractionations of RT with or without three fractions of  $\alpha$ CTLA4. The 8 Gy  $\times$  3 fractions treatment was used as the reference treatment, and different radiation dose fractionations (1, 2, 3, 5 or 10 fractions, one fraction per day, consecutive days) were studied, without IT, and in combination with three fractions of  $\alpha$ CTLA4 at days 2, 5 and 8 post-start of treatment. Doses associated to each fractionation were selected to have the same BED, calculated with  $\alpha_N/\beta_N = 39.6$  Gy

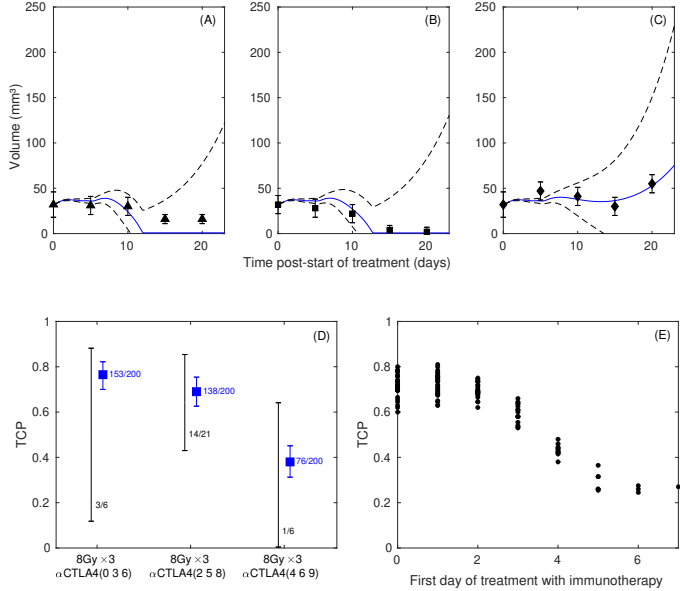


Fig. 6. Study of optimal schedules of administration of radiotherapy (8 Gy  $\times$  3 fractions) and immunotherapy (3 fractions of  $\alpha$ CTLA4) obtained with the biomathematical model and parameters reported in Supplementary Table 3. Radiotherapy fractions are delivered at days (0, 1, 2), and immunotherapy is delivered with different schedules starting from day 0 to day 7. In panels (A), (B) and (C) we report the dynamics of tumor volumes (mean  $\pm$  1 standard deviation) for three combinations that were investigated in [21], delivering immunotherapy at days (0, 3, 6), (2, 5, 8), and (4, 6, 9) respectively. In panel (D) we compare 95% confidence intervals for TCP values obtained with the model (200 simulations) and experimental controls (6 to 21 animals), for the same three treatment combinations. In (E) we present model TCPs versus the time of administration of the first IT fraction, showing that there is a negative correlation between those two variables if IT is delayed beyond two days post-start of RT.

(Supplementary Table 3). With this  $\alpha_N/\beta_N$  value, the doses per fraction for each fractionation were chosen as (for  $n$  fractions): 19.37 (1); 11.43 (2); 8 (3); 5.11 (5); 2.70 (10). Results are presented in Fig. 7, where we report evolution of tumor volumes under different treatment regimes, as well as tumor control probabilities (obtained as in the previous section, from 200 simulations with the stochastic Markov model described in Section 2.7, together with a relative normal random dispersion of best-fitting parameters of 10% to simulate population heterogeneity).

Conventional fractionation may be sub-standard, as daily fractions can deplete active T-cells from the tumor (it is widely assumed that T-cells are very radiosensitive, even though this idea may be contradicted by recent evidence [53]). In this regard, hypofractionated schedules may prove more effective (as already seen in some experimental studies), but without reaching extreme hypofractionation. In the latter case, the strategy may prove disadvantageous due to two factors: on the one hand, a single fraction may fail to keep therapeutic numbers of T-cells in the tumor for long times; on the other hand, very large doses may lose some effectiveness, and can seriously damage tumor vasculature, which limit the infiltration of active T-cells in the tumor, as previously investigated.

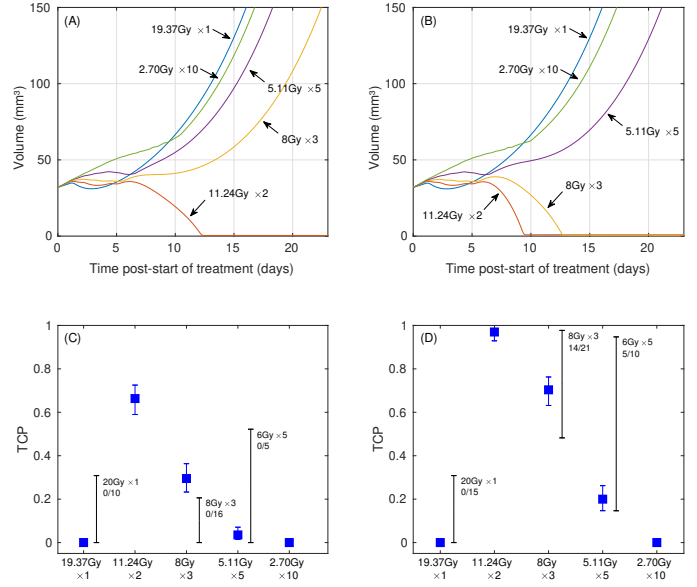


Fig. 7. Modeled responses to different radiotherapy schedules combined (or not) with three fractions of  $\alpha$ CTLA4 (at days 2, 5, and 8). Radiation schedules are iso-BED, and therefore equivalent from a classical radiobiological point of view, yet they lead to very different response curves due to the different interaction between radiation-induced cell death and immune-induced cell death. Tumor volume evolution is shown when treating with radiotherapy alone (A) and radiotherapy plus  $\alpha$ CTLA4. We also report tumor control probabilities (95% confidence intervals) obtained with the model (200 simulations) when simulating radiotherapy alone (C) and radiotherapy plus  $\alpha$ CTLA4 (D). Experimental TCP values are also presented for the most similar treatment strategies (notice that experimental and simulated doses differ). Model parameters used for this study are presented in Supplementary Table 3, and include vascular damage effect at 19.37 Gy (Equation (16)).

### 3.5 Sensitivity Analysis

In Table 1 we rank the sensitivity of the cost function to model parameters. The model is most sensitive to parameters describing tumor cell proliferation, radiosensitivity and immune-mediated tumor cell killing.

## 4 DISCUSSION

Radioimmunotherapy shows potential to improve cure rates in many cancer types. *In silico* mathematical models of tumor response to radioimmunotherapy can help to interpret experimental data, and ultimately may help to decide optimal therapeutic strategies. In this work we present a biomathematical model of tumor response to radioimmunotherapy with inhibitors of PD-L1 ( $\alpha$ PDL1) and CTLA-4 ( $\alpha$ CTLA4), which consists in a system of coupled impulsive delay differential equations to include biological response delays. Our approach follows an intermediate path between systems biology and phenomenological modeling, including a detailed description of the processes involved in response to radioimmunotherapy but without reaching the cellular/molecular scale of systems biology. We present the model in two flavors: on the one hand, a continuous/deterministic model, which is mainly used to fit experimental data of populational dynamics of tumor volumes; on the other hand, a stochastic/discrete model, obtained by treating the model as a Markov death/birth process, which is used to model tumor control probabilities.

The model can fit experimental tumor responses (evolution of tumor volumes) to different combinations of radiotherapy and immunotherapy with  $\alpha$ PDL1 and  $\alpha$ CTL4. It can also qualitatively reproduce experimental TCP values, even though the uncertainties of those values are large because they are obtained from a limited number of animals. One thing that our model fails to reproduce is the effect of  $\alpha$ PDL1 and  $\alpha$ CTL4 as monotherapy on progression of tumor volumes. While this effect is small in the collected experimental data (differences observed in a small number of animals are not significant), they show a consistent effect of IT alone on tumor volume. Our modeling results show no noticeable effect of  $\alpha$ CTL4 or  $\alpha$ PDL1 monotherapies. Therefore, the application of our model to IT monotherapies could be debatable. However, it might very well be that the low percentage of subjects responding to IT monotherapy treatments present a particular phenotype (model parameters) that makes them more sensitive to such therapies, and such effect cannot be reproduced when fitting population-averaged data.

The fits show very radio-resistant tumors (low  $\alpha$  values), but in line with reported experimental values for tumors in mice [54]. Interestingly, best fits are obtained when the relative radiosensitivity of the tumor cells decreases with increasing dose. This has been observed by fitting the data to a modified LQ-model that includes such behaviour, to the LQL model (which accounts for decreasing radiosensitivity through increasing repair), and also by limiting the infiltration of T-cells into the tumor due to vascular damage at large doses. All models lead to similar fits. We must notice that we have only included the effect of limited T-cell infiltration in this analysis for the sake of simplicity, but vascular damage may cause other effects, like proliferation arrest and starvation, resulting in a complex interaction.

Based on results obtained with our model, we can formulate hypotheses regarding the effectiveness of radioimmunotherapy. We have investigated the optimal schedule of administration of RT (8 Gy  $\times$  3) and IT (3 fractions). Our model indicates that a better synergy could be obtained by delivering IT soon after the first fraction of RT at the beginning of treatment, and the following IT fractions extending longer into the treatment, to keep therapeutic numbers of T-cell in the tumor for a longer time (according to the different kinetics of the IT drug, tumor cell death, and antigen liberation). The combined treatment starts to lose effectiveness if the administration of IT is delayed beyond two days post-start of RT.

We have also investigated optimal dose fractionation. Conventional fractionation of dose may be sub-optimal for radioimmunotherapy, but extreme hypofractionation may also prove suboptimal, either due to loss of effectiveness of such high-doses, or to critical damage to tumor vasculature that may limit T-cell infiltration. This might also explain the poorer results obtained with the 20 Gy single-fraction irradiation. Moderate hypofractionation of dose may offer the best results.

The combined study of what is usually called indirect tumor cell death in radiotherapy/radioimmunotherapy (due to vascular damage and radiation-triggered immune response) certainly seems to be of high importance, as they may interfere with each other. Biomathematical models

linking them can provide insight into the problem and help to interpret experimental results. Biomathematical modeling may also help to interpret conflicting experimental reports on the effect of indirect cell death on tumor response (for example, [15], [55], [56]). Compared to other models of immunotherapy/radioimmunotherapy response, in this work we present a simpler modeling of the immune-mediated tumor cell death, we explicitly include biological delays and evaluate their effect on optimal fractionation strategies, and we study the effect of indirect radiation cell damage (through vascular damage).

## 5 CONCLUSION

Biomathematical models that can help to interpret experimental data on the existent synergies between radiotherapy and immunotherapy, and to assist in the design of more effective radioimmunotherapies, could potentially boost the implementation of radioimmunotherapy. Such models may help to interpret and analyze clinical and pre-clinical data. From our work, it seems that a good understanding of the biological delays associated to such therapies, the biokinetics of the immunotherapy drug, and the interplay among them, may be of paramount importance to design optimal radioimmunotherapy schedules. Ultimately, we envision a key role for these models assisting in the design of more effective radioimmunotherapies, similarly to the role of the LQ model in conventional radiotherapy. Further work is required to create well-validated, but models like the one presented in this paper constitute a stepping stone towards that final goal.

## ACKNOWLEDGMENTS

We acknowledge the support of Instituto de Salud Carlos III through research grant PI17/01428 (FEDER co-fund). We acknowledge Dr. Viñuela from the Immunology Unit at the Clinical University Hospital of Santiago de Compostela for useful discussions.

## REFERENCES

- [1] T. Whiteside, S. Demaria, M. Rodriguez-Ruiz, H. Zarour, and I. Melero, "Emerging opportunities and challenges in cancer immunotherapy," *Clinical Cancer Research*, vol. 22, pp. 1845–1855, 2016.
- [2] T. Waldmann, "Immunotherapy: Past, present and future," *Nature Medicine*, vol. 9, pp. 269–277, 2003.
- [3] A. Scott, J. Wolchok, and L. Old, "Antibody therapy of cancer," *Nature Reviews Cancer*, vol. 12, pp. 278–287, 2012.
- [4] M. Postow, M. Callahan, C. Barker, Y. Yamada, J. Yuan, S. Kitano, Z. Mu, T. Rasalan, M. Adamow, E. Ritter, C. Sedrak, A. Jungbluth, R. Chua, A. Yang, R.-A. Roman, S. Rosner, B. Benson, J. Allison, A. Lesokhin, and J. Wolchok, "Immunologic correlates of the abscopal effect in a patient with melanoma," *The New England Journal of Medicine*, vol. 366, pp. 925–931, 2012.
- [5] E. Kwon, C. Drake, H. Scher, K. Fizazi, A. Bossi, A. Eertwegh, M. Krainer, H. Nadine, R. Santos, H. Mahammed, S. Ng, M. Maio, F. Franke, S. Sundar, N. Agarwal, A. Bergman, T. Ciuleanu, E. Korbenfeld, L. Sengelov, and W. Gerritsen, "Ipilimumab versus placebo after radiotherapy in patients with metastatic castration-resistant prostate cancer that had progressed after docetaxel chemotherapy (CA184-043): A multicentre, randomised, double-blind, phase 3 trial," *The Lancet Oncology*, vol. 15, pp. 700–712, 2014.

TABLE 1

Analysis of the most sensitive model parameters. The sensitivity index (28) for each parameter is calculated as the difference between the cost function of fits to experimental data presented in [21] (best-fitting parameters reported in Supplementary Table 3) and the cost function obtained when a 1% perturbation is applied to that particular parameter. Only the ten most sensitive parameters are shown. For reference, the cost function value obtained with best fitting parameters is 44.6971.

Parameter	Description [units]	Sensitivity
$q$	Immune-mediated tumor cell death parameter	3.1060
$\lambda_1$	Proliferation rate of tumor cells [days <sup>-1</sup> ]	1.2498
$\alpha_N$	Linear parameter of LQ model for tumor cells [Gy <sup>-1</sup> ]	0.4035
$T(t = 0)$	Initial pool of blank T-cells in activation site	0.4002
$p$	Immune-mediated tumor cell death rate [days <sup>-1</sup> ]	0.2775
$r$	Ratio of activation/inactivation rates	0.1821
$\iota$	Rate of death of T-cells due to interaction with tumor cells [days <sup>-1</sup> ]	0.0386
$\beta_N$	Quadratic parameter of LQ model for tumor cells [Gy <sup>-1</sup> ]	0.0212
$\psi$	Rate of release of antigens [days <sup>-1</sup> ]	0.0109
$a$	Rate of activation of T-cells [days <sup>-1</sup> ]	0.0109

[6] E. Golden, S. Demaria, P. Schiff, A. Chachoua, and S. Formenti, "An abscopal response to radiation and ipilimumab in a patient with metastatic non-small cell lung cancer," *Cancer Immunology Research*, vol. 1, pp. 365–372, 2013.

[7] L. Villaruz, A. Kalyan, H. Zarour, and M. Socinski, "Immunotherapy in lung cancer," *Translational Lung Cancer Research*, vol. 3, pp. 2–14, 2014.

[8] J. Gong, A. Chehrazi-Raffle, S. Reddi, and R. Salgia, "Development of PD-1 and PD-L1 inhibitors as a form of cancer immunotherapy: A comprehensive review of registration trials and future considerations," *Journal for ImmunoTherapy of Cancer*, vol. 6, p. 8, 2018.

[9] F. Hodi, S. O'Day, D. McDermott, R. Weber, J. Sosman, J. Hahn, R. Gonzalez, C. Robert, J. Hassel, W. Akerley, A. Eertwegh, J. Lutzky, P. Lorigan, J. Vaubel, G. Linette, D. Hogg, C. Ottensmeier, C. Lebbé, and W. Urba, "Improved survival with ipilimumab in patients with metastatic melanoma," *The New England Journal of Medicine*, vol. 363, pp. 711–723, 2010.

[10] M. Mondini, M. Nizard, T. Tran, L. Mauge, M. Loi, C. Clemenson, D. Dugue, P. Maroun, E. Louvet, J. Adam, C. Badoual, D. Helley, E. Dransart, L. Johannes, M.-C. Vozenin, J.-L. Perfettini, E. Tartour, and E. Deutsch, "Synergy of radiotherapy and a cancer vaccine for the treatment of HPV-associated head and neck cancer," *Molecular Cancer Therapeutics*, vol. 14, pp. 1336–1345, 2015.

[11] P. Sperduto, C. Song, J. Kirkpatrick, and E. Glatstein, "A hypothesis: Indirect cell death in the radiosurgery era," *International Journal of Radiation Oncology, Biology, Physics*, vol. 91, pp. 11–13, 2015.

[12] A. Levy, C. Chargini, A. Marabelle, J.-L. Perfettini, N. Magné, and E. Deutsch, "Can immunostimulatory agents enhance the abscopal effect of radiotherapy?" *European Journal of Cancer*, vol. 62, pp. 36–45, 2016.

[13] M. Crittenden, H. Kohrt, R. Levy, J. Jones, K. Camphausen, A. Dicker, S. Demaria, and S. Formenti, "Current clinical trials testing combinations of immunotherapy and radiation," *Seminars in Radiation Oncology*, vol. 25, pp. 54–64, 2015.

[14] E. Mladenov, S. Magin, A. Soni, and G. Iliakis, "DNA double-strand break repair as determinant of cellular radiosensitivity to killing and target in radiation therapy," *Frontiers in Oncology*, vol. 3, p. 113, 2013.

[15] C. Song, Y.-J. Lee, R. Griffin, I. Park, N. Koonce, S. Hui, M.-S. Kim, K. Dusenberry, P. Sperduto, and L. Cho, "Indirect tumor cell death after high dose hypo-fractionated irradiation: Implications for SBRT and SRS," *International Journal of Radiation Oncology\*Biology\*Physics*, vol. 93, pp. 166–172, 2015.

[16] C. W. Song, H. Park, R. J. Griffin, and S. H. Levitt, *Radiobiology of Stereotactic Radiosurgery and Stereotactic Body Radiation Therapy*. Berlin, Heidelberg: Springer Berlin Heidelberg, 2012.

[17] L. Cruz-Merino, A. Vacas, A. Grueso-López, A. Sánchez, and C. Míguez-Sánchez, "Radiation for awakening the dormant immune system, a promising challenge to be explored," *Frontiers in Immunology*, vol. 5, p. 102, 2014.

[18] D. Chen and I. Mellman, "Oncology meets immunology: The cancer-immunity cycle," *Immunity*, vol. 39, pp. 1–10, 2013.

[19] F. Herrera, J. Bourhis, and G. Coukos, "Radiotherapy combination opportunities leveraging immunity for the next oncology practice: Radiation-immunotherapy combinations," *CA: A Cancer Journal for Clinicians*, vol. 67, pp. 65–85, 2016.

[20] T. Walle, R. Martinez-Monge, A. Cerwenka, D. Ajona, I. Melero, and F. Lecanda, "Radiation effects on antitumor immune responses: Current perspectives and challenges," *Therapeutic Advances in Medical Oncology*, vol. 10, p. 1758834017742575, 2018.

[21] M. Dewan, A. Galloway, N. Kawashima, J. Dewyngaert, J. Babb, S. Formenti, and S. Demaria, "Fractionated but not single-dose radiotherapy induces an immune-mediated abscopal effect when combined with anti-CTLA-4 antibody," *Clinical Cancer Research*, vol. 15, pp. 5379–5388, 2009.

[22] L. Deng, H. Liang, B. Burnette, M. Beckett, T. Darga, R. Weichselbaum, and Y.-X. Fu, "Irradiation and anti-PD-L1 treatment synergistically promote antitumor immunity in mice," *The Journal of Clinical Investigation*, vol. 124, pp. 687–695, 2014.

[23] L. Depillis, A. Radunskaya, and C. Wiseman, "A validated mathematical model of cell-mediated immune response to tumor growth," *Cancer Research*, vol. 65, pp. 7950–7958, 2005.

[24] L. Depillis, W. Gu, and A. Radunskaya, "Mixed immunotherapy and chemotherapy of tumors: Modeling, applications and biological interpretations," *Journal of Theoretical Biology*, vol. 238, pp. 841–862, 2006.

[25] S. Chareyron and M. Alamir, "Mixed immunotherapy and chemotherapy of tumors: feedback design and model updating schemes," *Journal of Theoretical Biology*, vol. 258, pp. 444–454, 2009.

[26] L. Xiulan and A. Friedman, "Combination therapy of cancer with cancer vaccine and immune checkpoint inhibitors: A mathematical model," *PLoS ONE*, vol. 12, p. e0178479, 2017.

[27] A. Radunskaya, R. Kim, and T. II, "Mathematical modeling of tumor immune interactions: a closer look at the role of a PD-L1 inhibitor in cancer immunotherapy," *SPORA: A Journal of Biomathematics*, vol. 4, pp. 25–41, 2018.

[28] M. Benchaib, A. Bouchnita, V. Volpert, and A. Makhoute, "Mathematical modeling reveals that the administration of EGF can promote the elimination of lymph node metastases by PD-1/PD-L1 blockade," *Frontiers in Bioengineering and Biotechnology*, vol. 7, p. 104, 2019.

[29] R. Eftimie, J. Bramson, and D. Earn, "Interactions between the immune system and cancer: A brief review of non-spatial mathematical models," *Bulletin of Mathematical Biology*, vol. 73, pp. 2–32, 2011.

[30] R. Serre, S. Benzekry, L. Padovani, C. Meille, N. Andre, J. Ciccolini, F. Barlesi, X. Muracciole, and D. Barbolosi, "Mathematical modeling of cancer immunotherapy and its synergy with radiotherapy," *Cancer Research*, vol. 76, pp. 4931–4940, 2016.

[31] R. Serre, F. Barlesi, X. Muracciole, and D. Barbolosi, "Immunologically effective dose: A practical model for immuno-radiotherapy," *Oncotarget*, vol. 9, pp. 31 812–31 819, 2018.

[32] Y. Kosinsky, S. Dovedi, K. Peskov, V. Voronova, L. Chu, H. Tomkinson, N. Al-Huniti, D. Stanski, and G. Helmlinger, "Radiation and PD-(L)1 treatment combinations: Immune response and dose

optimization via a predictive systems model," *Journal for Immunotherapy of Cancer*, vol. 6, p. 17, 2018.

[33] J. Polesczuk and H. Enderling, "The optimal radiation dose to induce robust systemic anti-tumor immunity," *International Journal of Molecular Sciences*, vol. 19, p. 3377, 2018.

[34] W. Sung, C. Grassberger, A. McNamara, L. Basler, S. Ehrbar, S. Tanadini-Lang, T. Hong, and H. Paganetti, "A tumor-immune interaction model for hepatocellular carcinoma based on measured lymphocyte counts in patients undergoing radiotherapy," *Radiotherapy and Oncology*, vol. 151, pp. 73–81, 2020.

[35] J. Butner, D. Elgarnainy, C. Wang, Z. Wang, S.-H. Chen, N. Esnaola, R. Pasqualini, W. Arap, D. Hong, J. Welsh, E. Koay, and V. Cristini, "Mathematical prediction of clinical outcomes in advanced cancer patients treated with checkpoint inhibitor immunotherapy," *Science Advances*, vol. 6, p. eaay6298, 2020.

[36] B. Wouters and J. Brown, "Cells at intermediate oxygen levels can be more important than the "hypoxic fraction" in determining tumor response to fractionated radiotherapy," *Radiation Research*, vol. 147, pp. 541–550, 1997.

[37] J. Kirkpatrick, J. Meyer, and L. Marks, "The linear-quadratic model is inappropriate to model high dose per fraction effects in radiosurgery," *Seminars in Radiation Oncology*, vol. 18, pp. 240–243, 2008.

[38] A. Gago-Arias, S. Neira, M. Pombar, A. Gómez-Caamaño, and J. Pardo-Montero, "Evaluation of indirect damage and damage saturation effects in dose-response curves of hypofractionated radiotherapy of early-stage NSCLC and brain metastases," *Radiotherapy and Oncology*, vol. 160, p. IN PRESS, 2021.

[39] M. Guerrero and X. Li, "Extending the linear-quadratic model for large fraction doses pertinent to stereotactic radiotherapy," *Physics in Medicine and Biology*, vol. 49, pp. 4825–4835, 2004.

[40] A. Gago-Arias, P. Aguiar, I. Espinoza, B. Sanchez, and J. Pardo-Montero, "Modelling radiation-induced cell death and tumour re-oxygenation: Local versus global and instant versus delayed cell death," *Physics in Medicine and Biology*, vol. 61, pp. 1204–1216, 2016.

[41] S. Fedotov and A. Iomin, "Probabilistic approach to a proliferation and migration dichotomy in tumor cell invasion," *Physical Review E*, vol. 77, p. 031911, 2008.

[42] W. Dorr, "Three a's of repopulation during fractionated irradiation of squamous epithelia: asymmetry loss, acceleration of stem-cell divisions and abortive divisions," *International Journal of Radiation Biology*, vol. 72, pp. 635–643, 1997.

[43] P. Rodríguez-Barbeito, P. Díaz-Botana, A. Gago-Arias, M. Feijoo, S. Neira, J. Guiu-Souto, O. López Pouso, A. Gómez-Caamaño, and J. Pardo-Montero, "A model of indirect cell death caused by tumor vascular damage after high-dose radiotherapy," *Cancer Research*, vol. 79, pp. 6044–6053, 2019.

[44] M. Selby, J. Engelhardt, M. Quigley, K. Henning, T. Chen, M. Srinivasan, and A. Korman, "Anti-CTLA-4 antibodies of IgG2a isotype enhance antitumor activity through reduction of intratumoral regulatory T cells," *Cancer Immunology Research*, vol. 1, pp. 32–42, 2013.

[45] R. Deng, D. Bumbaca, C. Pastuskovas, C. Boswell, D. West, K. Cowan, H. Chiu, J. McBride, C. Johnson, Y. Xin, H. Koeppen, M. Leabman, and S. Iyer, "Preclinical pharmacokinetics, pharmacodynamics, tissue distribution, and tumor penetration of anti-PD-L1 monoclonal antibody, an immune checkpoint inhibitor," *mAbs*, vol. 8, pp. 593–603, 2016.

[46] S. Webb and A. Nahum, "A model for calculating tumour control probability in radiotherapy including the effects of inhomogeneous distributions of dose and clonogenic cell density," *Physics in Medicine and Biology*, vol. 38, pp. 653–666, 1993.

[47] L. Hanin, "Iterated birth and death process as a model of radiation cell survival," *Mathematical Biosciences*, vol. 169, pp. 89–107, 2001.

[48] S. Kirkpatrick, C. Gelatt, and M. Vecchi, "Optimization by simulated annealing," *Science*, vol. 220, pp. 671–680, 1983.

[49] B. Jones, R. Dale, C. Deehan, K. Hopkins, and D. Morgan, "The role of biologically effective dose (BED) in clinical oncology," *Clinical oncology (Royal College of Radiologists (Great Britain))*, vol. 13, pp. 71–81, 2001.

[50] W. H. Press, S. A. Teukolsky, W. T. Vetterling, and B. P. Flannery, *Numerical Recipes 3rd Edition: The Art of Scientific Computing*, 3rd ed. USA: Cambridge University Press, 2007.

[51] I. González-Crespo, A. Gómez-Caamaño, O. López Pouso, and J. Pardo-Montero, "Replication data for "a biomathematical model of tumor response to radioimmunotherapy with  $\alpha$ PDL1 and  $\alpha$ CTLA4"," 2019. [Online]. Available: <https://doi.org/10.7910/DVN/QE2TKH>

[52] R. Kuse, S. Schuster, H. Schübbe, S. Dix, and K. Hausmann, "Blood lymphocyte volumes and diameters in patients with chronic lymphocytic leukemia and normal controls," *Blut*, vol. 50, p. 243–248, 1985.

[53] A. Arina, M. Beckett, C. Fernandez, W. Zheng, S. Pitroda, S. Chmura, J. Luke, M. Forde, Y. Hou, B. Burnette, H. Mauceri, I. Lowy, T. Sims, N. Khodarev, Y.-X. Fu, and R. Weichselbaum, "Tumor-reprogrammed resident T cells resist radiation to control tumors," *Nature Communications*, vol. 10, p. 3959, 2019.

[54] C. van Leeuwen, A. Oei, H. Crezee, A. Bel, N. Franken, L. Stalpers, and H. Kok, "The alfa and beta of tumours: A review of parameters of the linear-quadratic model, derived from clinical radiotherapy studies," *Radiation Oncology*, vol. 13, p. 96, 2018.

[55] E. J. Moding, K. D. Castle, B. Perez, P. Oh, H. D. Min, H. Norris, Y. Ma, D. Cardona, C.-L. Lee, and D. Kirsch, "Tumor cells, but not endothelial cells, mediate eradication of primary sarcomas by stereotactic body radiation therapy," *Science Translational Medicine*, vol. 7, p. 278ra34, 2015.

[56] J. Torok, P. Oh, K. Castle, M. Reinsvold, Y. Ma, L. Luo, C.-L. Lee, and D. Kirsch, "Deletion of atm in tumor but not endothelial cells improves radiation response in a primary mouse model of lung adenocarcinoma," *Cancer Research*, vol. 79, pp. 7773–7782, 2018.

TABLE Supplementary 1

List of best-fitting parameters of our model to experimental data reported in references [21] and [22]. A modified LQ-model was used to account for tumor cell radiosensitivity (Equations (1) and (2)). The symbol \* indicates that the parameter value was fixed and not included in the optimization, while \*\* indicates that the parameter was optimized, but the same value was used for  $\alpha$ CTLA4 and  $\alpha$ PDL1 fitting. *Dewan* and *Deng* refer to best-fitting parameters to data reported in [21] and [22], respectively. Initial numbers/concentrations of variables not indicated in the table ( $N_d$ ,  $A$ ,  $L$ ,  $T_p$ ,  $T_m$ ,  $c_4$ ,  $p_1$ ) are set to zero.

Parameters/Initial conditions		
Parameter	Description [units]	Value
$N(t = 0)$	*Initial number of tumor cells	100
$T(t = 0)$	**Initial pool of <i>blank</i> T-cells in activation site	$1.5145 \times 10^7$
$\lambda_1$	Proliferation rate of tumor cells [days $^{-1}$ ]	0.1476 (Dewan), 0.1517 (Deng)
$\lambda_2$	Saturation of proliferation	$6.0573 \times 10^{-10}$ (Dewan), $1.1164 \times 10^{-9}$ (Deng)
$\alpha_N$	Linear parameter of LQ model for tumor cells [Gy $^{-1}$ ]	0.0186 (Dewan), 0.0445 (Deng)
$\beta_N$	Quadratic parameter of LQ model for tumor cells [Gy $^{-2}$ ]	0.0068 (Dewan), 0.0014 (Deng)
$c$	Modulation factor of the $\beta_N$ parameter [Gy $^{-1/2}$ ]	$-0.2118$ (Dewan), $-2.4027 \times 10^{-14}$ (Deng)
$\phi$	**Rate of elimination of doomed tumor cells [days $^{-1}$ ]	0.4579
$\tau_{d1}$	*Mitotic delay (start) [days]	1
$\tau_{d2}$	*Mitotic delay (end) [days]	1.5000
$p$	**Immune-mediated tumor cell death rate [days $^{-1}$ ]	12.0881
$q$	**Immune-mediated tumor cell death parameter	1.3985
$s$	**Slope of the immune-mediated tumor death curve	$4.2253 \times 10^{-4}$
$i_{p1}$	Dose of $\alpha$ PDL1 per fraction	8.3606 (if $\alpha$ PDL1), 0 (otherwise)
$\mu$	*Rate of elimination of $\alpha$ PDL1 [days $^{-1}$ ]	0.5000
$\rho$	**Rate of natural production of antigens [days $^{-1}$ ]	$3.5345 \times 10^{-8}$
$\psi$	**Rate of release of antigens [days $^{-1}$ ]	22.6042
$\tau_1$	**Delay between antigen liberation and T-cell activation [days]	1.1585
$\sigma$	**Rate of natural elimination of antigens [days $^{-1}$ ]	$1.2618 \times 10^{-5}$
$a$	**Rate of activation of T-cells [days $^{-1}$ ]	$8.5265 \times 10^{-10}$
$r$	**Ratio of activation/inactivation rates	1.9869
$i_{c4}$	Dose of $\alpha$ CTLA4 per fraction	3.5630 (if $\alpha$ CTLA4), 0 (otherwise)
$\nu$	*Rate of elimination of $\alpha$ CTLA4 [days $^{-1}$ ]	0.1000
$\tau_2$	**Time taken by activated T-cell to reach the tumor [days]	2.3473
$\alpha_L$	**Linear parameter of LQ model for T-cells [Gy $^{-1}$ ]	$5.3462 \times 10^{-7}$
$\beta_L$	**Quadratic parameter of LQ model for T-cells [Gy $^{-2}$ ]	$5.3462 \times 10^{-8}$
$\iota$	**Rate of death of T-cells due to interaction with tumor cells [days $^{-1}$ ]	$1.3811 \times 10^{-8}$
$\eta$	**Rate of natural elimination of T-cells [days $^{-1}$ ]	$1.2330 \times 10^{-8}$
$h$	**Rate of production of <i>blank</i> T-cells [days $^{-1}$ ]	$1.6014 \times 10^{-13}$
$V_N$	*Volume of tumor cells [mm $^3$ ]	$10^{-6}$
$V_L$	*Volume of T-cells [mm $^3$ ]	$2 \times 10^{-7}$

TABLE Supplementary 2

List of best-fitting parameters of our model to experimental data reported in reference [21]. The LQL model was used to account for tumor cell radiosensitivity (Equation (3)). The symbol \* indicates that the parameter value was fixed and not included in the optimization. Initial numbers/concentrations of variables not indicated in the table ( $N_d$ ,  $A$ ,  $L$ ,  $T_p$ ,  $T_m$ ,  $c_4$ ,  $p_1$ ) are set to zero.

Parameters/Initial conditions		
Parameter	Description [units]	Value
$N(t = 0)$	*Initial number of tumor cells	100
$T(t = 0)$	Initial pool of <i>blank</i> T-cells in activation site	$4.4916 \times 10^8$
$\lambda_1$	Proliferation rate of tumor cells [days $^{-1}$ ]	0.1303
$\lambda_2$	Saturation of proliferation	$1.9313 \times 10^{-22}$
$\alpha_N$	Linear parameter of LQ model for tumor cells [Gy $^{-1}$ ]	0.0443
$\beta_N$	Quadratic parameter of LQ model for tumor cells [Gy $^{-2}$ ]	$6.6376 \times 10^{-4}$
$x$	Modulation factor of the $\beta_N$ parameter [Gy $^{-1/2}$ ]	0.1052
$\phi$	Rate of elimination of doomed tumor cells [days $^{-1}$ ]	0.1234
$\tau_{d1}$	*Mitotic delay (start) [days]	1
$\tau_{d2}$	*Mitotic delay (end) [days]	1.5
$p$	Immune-mediated tumor cell death rate [days $^{-1}$ ]	0.6814
$q$	Immune-mediated tumor cell death parameter	3.3580
$s$	Slope of the immune-mediated tumor death curve	$1.9428 \times 10^{-12}$
$\rho$	Rate of natural production of antigens [days $^{-1}$ ]	$1.3487 \times 10^{-18}$
$\psi$	Rate of release of antigens [days $^{-1}$ ]	9.8790
$\tau_1$	Delay between antigen liberation and T-cell activation [days]	1.9943
$\sigma$	Rate of natural elimination of antigens [days $^{-1}$ ]	$1.0593 \times 10^{-21}$
$a$	Rate of activation of T-cells [days $^{-1}$ ]	$1.3895 \times 10^{-9}$
$r$	Ratio of activation/inactivation rates	10
$i_{c4}$	Dose of $\alpha$ CTLA4 per fraction	947.6260
$\nu$	*Rate of elimination of $\alpha$ CTLA4 [days $^{-1}$ ]	0.1000
$\tau_2$	Time taken by activated T-cell to reach the tumor [days]	$3.8313 \times 10^{-7}$
$\alpha_L$	Linear parameter of LQ model for T-cells [Gy $^{-1}$ ]	$8.7536 \times 10^{-17}$
$\beta_L$	Quadratic parameter of LQ model for T-cells [Gy $^{-2}$ ]	$8.7536 \times 10^{-18}$
$\iota$	Rate of death of T-cells due to interaction with tumor cells [days $^{-1}$ ]	$4.2868 \times 10^{-8}$
$\eta$	Rate of natural elimination of T-cells [days $^{-1}$ ]	$4.8407 \times 10^{-11}$
$h$	Rate of production of <i>blank</i> T-cells [days $^{-1}$ ]	$2.4905 \times 10^{-20}$
$V_N$	*Volume of tumor cells [mm $^3$ ]	$10^{-6}$
$V_L$	*Volume of T-cells [mm $^3$ ]	$2 \times 10^{-7}$

TABLE Supplementary 3

List of best-fitting parameters of our model to experimental data reported in reference [21]. The LQ model was used to account for tumor cell radiosensitivity (Equation (1)), and limited T-cell infiltration was assumed for 20 Gy irradiation due to vascular damage (Equation (16)). The symbol \* indicates that the parameter value was fixed and not included in the optimization. Initial numbers/concentrations of variables not indicated in the table ( $N_d$ ,  $A$ ,  $L$ ,  $T_p$ ,  $T_m$ ,  $c_4$ ,  $p_1$ ) are set to zero.

Parameters/Initial conditions		
Parameter	Description [units]	Value
$N(t = 0)$	*Initial number of tumor cells	100
$T(t = 0)$	Initial pool of <i>blank</i> T-cells in activation site	$7.1610 \times 10^6$
$\lambda_1$	Proliferation rate of tumor cells [ $\text{days}^{-1}$ ]	0.1350
$\lambda_2$	Saturation of proliferation	$4.7265 \times 10^{-17}$
$\alpha_N$	Linear parameter of LQ model for tumor cells [ $\text{Gy}^{-1}$ ]	0.0212
$\beta_N$	Quadratic parameter of LQ model for tumor cells [ $\text{Gy}^{-2}$ ]	$5.3471 \times 10^{-4}$
$\phi$	Rate of elimination of doomed tumor cells [ $\text{days}^{-1}$ ]	0.5996
$\tau_{d1}$	*Mitotic delay (start) [days]	1
$\tau_{d2}$	*Mitotic delay (end) [days]	1.5000
$p$	Immune-mediated tumor cell death rate [ $\text{days}^{-1}$ ]	14.9308
$q$	Immune-mediated tumor cell death parameter	1.2824
$s$	Slope of the immune-mediated tumor death curve	0.0071
$\rho$	Rate of natural production of antigens [ $\text{days}^{-1}$ ]	$7.7438 \times 10^{-11}$
$\psi$	Rate of release of antigens [ $\text{days}^{-1}$ ]	160.1541
$\tau_1$	Delay between antigen liberation and T-cell activation [days]	$1.8119 \times 10^{-13}$
$\sigma$	Rate of natural elimination of antigens [ $\text{days}^{-1}$ ]	$6.3748 \times 10^{-11}$
$a$	Rate of activation of T-cells [ $\text{days}^{-1}$ ]	$2.1677 \times 10^{-11}$
$r$	Ratio of activation/inactivation rates	2.2126
$i_{c4}$	Dose of $\alpha$ CTLA4 per fraction	3.4325
$\nu$	*Rate of elimination of $\alpha$ CTLA4 [ $\text{days}^{-1}$ ]	0.1000
$\tau_2$	Time taken by activated T-cell to reach the tumor [days]	2.5958
$\alpha_L$	Linear parameter of LQ model for T-cells [ $\text{Gy}^{-1}$ ]	$4.0562 \times 10^{-9}$
$\beta_L$	Quadratic parameter of LQ model for T-cells [ $\text{Gy}^{-2}$ ]	$4.0562 \times 10^{-10}$
$\iota$	Rate of death of T-cells due to interaction with tumor cells [ $\text{days}^{-1}$ ]	$3.1611 \times 10^{-9}$
$\eta$	Rate of natural elimination of T-cells [ $\text{days}^{-1}$ ]	$1.3129 \times 10^{-13}$
$h$	Rate of production of <i>blank</i> T-cells [ $\text{days}^{-1}$ ]	$1.6014 \times 10^{-13}$
$V_N$	*Volume of tumor cells [ $\text{mm}^3$ ]	$10^{-6}$
$V_L$	*Volume of T-cells [ $\text{mm}^3$ ]	$2 \times 10^{-7}$

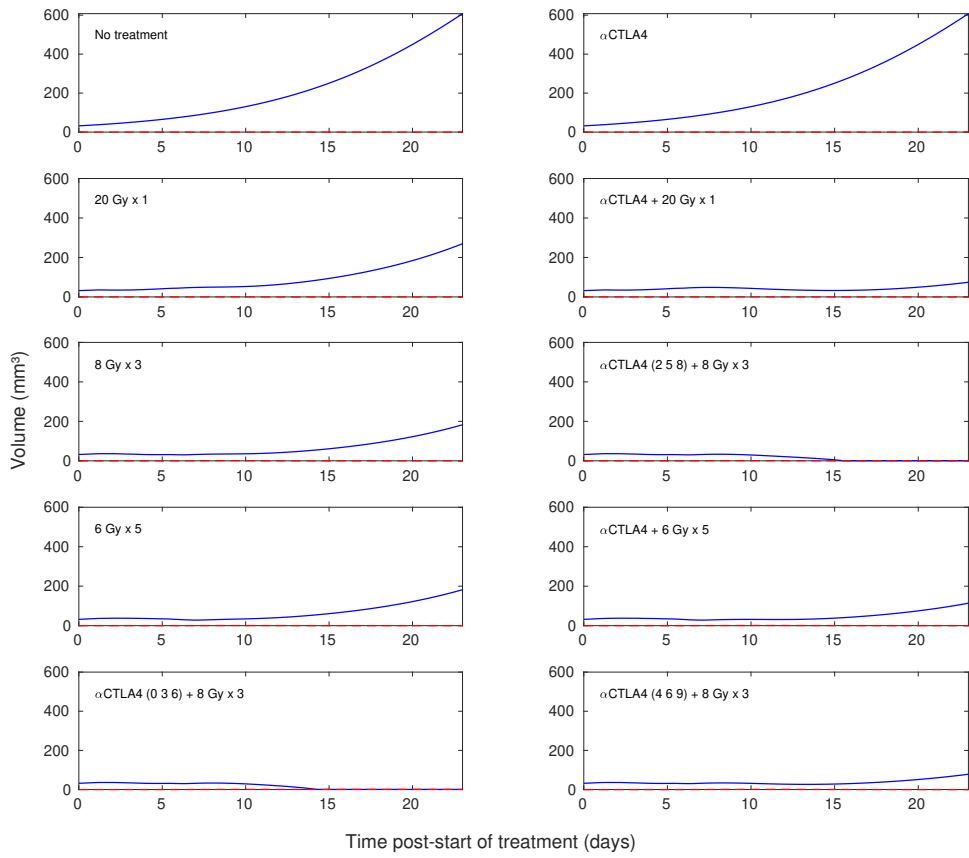


Fig. Supplementary 1. Contribution of tumor cells (solid lines) and T-cells (dashed lines) to tumor volumes in fits of our biomathematical model to experimental data reported by Dewan et al. [21]. Tumor volumes are dominated by tumor cells.

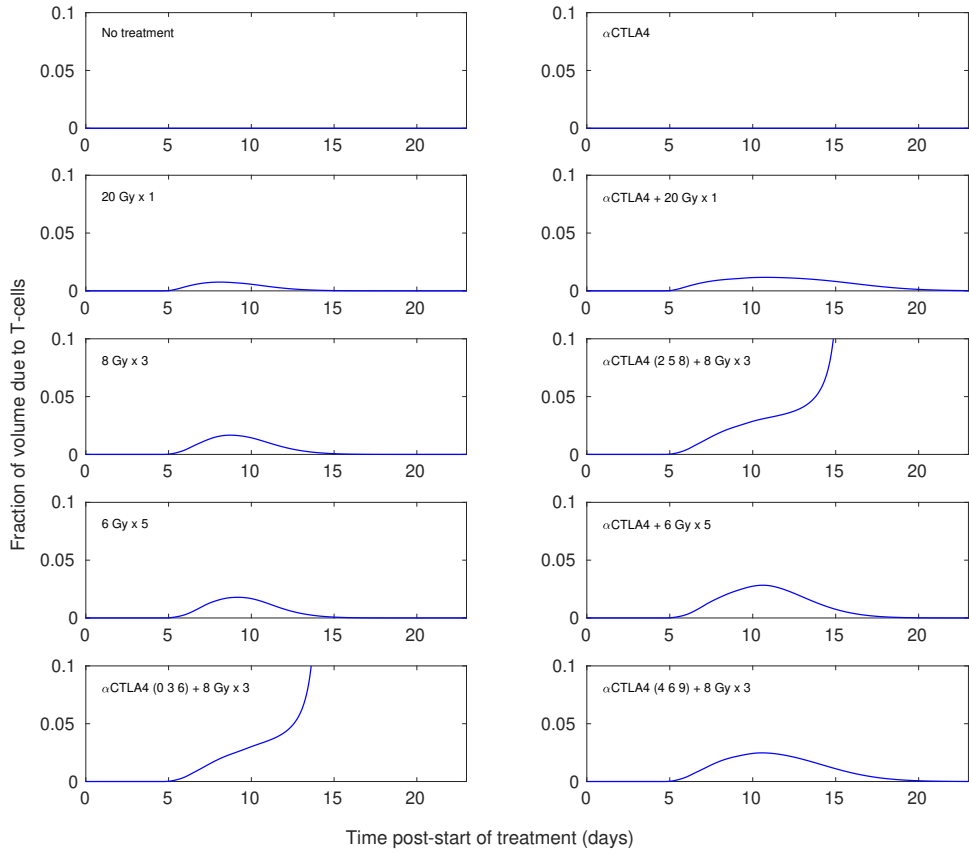


Fig. Supplementary 2. Relative contribution of T-cells (dashed lines) to tumor volumes in fits of our biomathematical model to experimental data reported by Dewan et al. [21]. Tumor volumes are dominated by tumor cells, and only when the tumor is close to remission the fraction of T-cells becomes large.